Ray, R., Holick, S. A., & Holick, M. F. (1985a) *J. Chem. Soc., Chem. Comm. 11*, 702-703.
Ray, R., Rose, S., Holick, S. A., & Holick, M. F. (1985b) *Biochem. Biophys. Res. Commun. 132*, 198-203.
Ray, R., Holick, S. A., Hanafin, N., & Holick, M. F. (1986) *Biochemistry 25*, 4729-4733.
Ray, R., Bouillon, R., Van Baelen, H., & Holick, M. F. (1991) *Biochemistry 30*, 4809-4813.
Schoentgen, F., Metz-Boutigue, M., Jolles, J., Constans, J., & Jolles, P. (1986) *Biochem. Biophys. Acta. 871*, 189-198.
Skinner, R. K., & Wills, M. R. (1977) *Clin. Chim. Acta 80*, 543-554.
Sweet, F., & Murdock, G. L. (1987) *Endocr. Rev. 8*, 154-184.
Van Baelen, H., & Bouillon, R. (1986) in *Binding Proteins of Steroid Hormones* (Forest, M. G., & Pugeat, M., Eds.) Vol. 149, pp 69-83, John Libbey Eurotext Ltd., London.
Van Baelen, H., Bouillon, R., & DeMoor, P. (1980) *J. Biol. Chem. 255*, 2270-2272.
Williams, M. H., Van Alstyne, E. L., & Galbraith, R. M. (1988) *Biochem. Biophys. Res. Commun. 153*, 1019.
Yang, F., Brune, J. I., Naylor, S. L., Cupples, R. L., Naberhaus, K. H., & Bowman, B. H. (1985a) *Proc. Natl. Acad. Sci. U.S.A. 82*, 7994-7998.
Yang, F., Luna, V. J., McAnelly, R. D., Naberhaus, K. H., Cupples, R. L., & Bowman, B. H. (1985b) *Nucleic Acids Res. 13*, 8007.

Fluorescence Studies on the Interactions of Myelin Basic Protein in Electrolyte Solutions†

Mark W. Nowak and Harvey Alan Berman*
Department of Biochemical Pharmacology, State University of New York at Buffalo, Buffalo, New York 14260
Received January 18, 1991; Revised Manuscript Received April 18, 1991

ABSTRACT: This paper examines the influence of electrolytes on fluorescence spectral properties of the single tryptophanyl residue, Trp-115, within the 18.5-kDa species of myelin basic protein from bovine brain. Steady-state fluorescence spectra and intensities and time-correlated fluorescence lifetimes increased in the presence of increasing concentrations of mono- and divalent electrolytes (Li^+, Na^+, K^+, Mg^{2+}, Ca^{2+}, Cl^-, ClO_4^-, SO_4^{2-}, and PO_4^{3-}). In all cases, the increases closely paralleled the ionic strength of the bulk aqueous medium and resembled that observed upon immersion of the protein in solutions of urea. This behavior was therefore concluded to reflect changes in the solution conformation of myelin basic protein. Bimolecular quenching of Trp-115 by acrylamide was rapid (10^9 M^{-1} s^{-1}), approaching the diffusion limitation, and markedly dependent on the viscosity of the bulk aqueous medium. Rotational depolarization of myelin basic protein was rapid ($\phi \leq 1$ ns), occurring at rates exceeding those predicted for a rigid particle of revolution, and markedly dependent on the viscosity of the surrounding medium. Whereas the bimolecular quenching constants were unaltered in the presence of electrolytes, rotational depolarization of myelin basic protein underwent substantial slowing as indicated by the appearance of an additional decay component characterized by a correlation time of 5-10 ns. These studies indicate that Trp-115 of myelin basic protein is readily accessible to the bulk aqueous medium and is associated with a highly mobile segment of the protein. The slowing of rotational depolarization upon immersion of myelin basic protein in electrolyte solutions is consistent with an electrolyte-induced self-association of myelin basic protein molecules and indicates a relationship between the lability of solution conformation on the one hand and the capacity for self-association on the other.

Myelin basic proteins are a class of cytoplasmic species that are synthesized in Schwann cells and oligodendrocytes and are present in myelin as physically distinct molecular forms of differing molecular weights. These species arise through alternative splicing of a single primary gene transcript (de Ferra et al., 1985; Kamholz et al., 1986, 1988; Lemke, 1988; Campagnoni & Macklin, 1988), are uniformly small, appearing as 14-, 17-, 18.5-, and 21-kDa species, and highly basic, with isoelectric points estimated to be greater than 10, and are required for myelination (Lemke, 1988). They are localized to the cytoplasmic appositions, referred to as *major dense lines*, and are therefore confined to the interior of the cell. As a consequence of their highly basic properties, it might be expected that the ionic composition of the cytoplasmic environment influences myelin basic protein with respect to conformation and function.

This question is of interest in that unlike a number of enzyme species, for which functional responses can be examined under differing physical conditions, myelin basic protein displays no readily discernible functional index. It is clear that myelin basic protein is required for normal myelination within the central nervous system. While the genetics underlying expression of myelin basic protein are becoming increasingly understood (Lemke, 1988; Campagnoni & Macklin, 1988), the physical determinants governing its structure and function with respect to the wrapping and compaction of myelin remain unknown. What is known is that, as discerned from studies of intrinsic viscosity (Epand et al., 1974), low-angle X-ray scattering (Krigbaum & Hsu, 1975), and circular dichroism (Gow & Smith, 1989), myelin basic protein in solution displays a near-random-coil configuration and a concentration-dependent capacity to undergo self-association in the absence

† This work was supported by grants from the National Institutes of Health (ES-03085) and the U.S. Army Research Office, Research Triangle Park, NC.

0006-2960/91/0430-7642$02.50/0 © 1991 American Chemical Society

and presence of micelle-forming detergents (Smith, 1980: Moskaitis et al., 1987; Lampe et al., 1983; Young et al., 1982). While such behavior is known, the trigger or physical mechanisms that initiate such protein–protein and protein–lipid interactions are unknown.

This paper examines myelin basic protein (MBP)[1] with respect to its behavior in solution and its responses to changes in ionic composition of the surrounding medium. The 18.5-kDa species from bovine brain is chosen for study since, of the myelin basic protein molecular forms, this species is the most abundant and contains a single tryptophanyl residue, Trp-115 (Less & Brostoff, 1984), rendering it ideal for spectroscopic investigation. Moreover, Trp-115 is advantageous for study since it is located within the *central region* of the myelin basic protein primary sequence. This central region, comprising residues 81–118, is highly conserved among mammalian species (Brostoff, 1984) and contains the antigenic determinant for experimental allergic encephalomyelitis in guinea pig and rabbit (Hung & Rauch, 1979) and sites for posttranslational phosphorylation and methylation (Martenson et al., 1983; Baldwin & Carnegie, 1971; Miyake, 1975; Young et al., 1987). While the hydrodynamic behavior of MBP is consistent with a random-coil conformation, the central region is inferred to contain at least a small degree of secondary structure since, of the 18 arginine residues contained in the primary sequence, posttranslational methylation occurs at only a single residue, Arg-106. In addition, this central region contains an unusual triprolyl sequence (Pro^{95}-Arg-Thr-Pro-Pro-Pro^{100}) that appears to form local hairpin tuns (Lees & Brostoff, 1984).

The dependence of the microscopic environment and accessibility of the Trp-115 residue on the ionic composition of the medium is examined by employing techniques of steady-state and time-correlated fluorescence spectroscopy, anisotropy decay, and bimolecular energy transfer in solution. Results obtained for MBP are compared with those obtained from human serum albumin (HSA) and *N*-acetyltryptophanamide (NATA). HSA, a globular protein of 66-kDa molecular mass, is chosen as a frame of reference because it also contains a single tryptophanyl residue and provides a suitable comparison for the considerably smaller MBP.

Materials and Methods

Materials. *N*-Acetyltryptophanamide, human serum albumin (Sigma Chemical Co.), and acrylamide (>99% purity; Bio-Rad) were used without further purification. (Carboxymethyl)cellulose (CM-52) and (diethylaminoethyl)cellulose (DE-52) were obtained from Whatman, Inc. All salts and solvents were obtained from commercially available sources. Bovine brain was obtained fresh from a local abattoir immediately prior to use.

Myelin Basic Protein. MBP was acid-extracted from fresh bovine brain as described by Deibler et al. (1984). A portion of the crude acid extract (200 mg), dissolved in 0.05 M glycine buffer, pH 10.6, containing 2 M urea, was applied to a CM-52 column (2.5 × 18.5 cm) equilibrated with the same buffer and eluted with a linear NaCl gradient (0–0.3 M). The protein peak was dialyzed against 50 volumes of distilled H_2O and lyophilized. Purity of the fractions was assessed by SDS–PAGE (Laemmeli, 1971). Gels stained with Coomassie blue R-250 showed a prominent band corresponding to the 18.5-kDa species of MBP and two very faint bands of 26 and 44 kDa. The yield of MBP was approximately 0.75–1.0 mg/g wet weight of white matter.

[1] Abbreviations: MBP, myelin basic protein; HSA, human serum albumin; NATA, *N*-acetyltryptophanamide.

Spectroscopy. Fluorescence emission spectra were obtained on a SPEX 212 fluorescence spectrometer equipped with a 450-W xenon light source, cooled photon counting detection, and a hamamatsu R928P photomultiplier tube. Steady-state titrations were carried out on an Aminco-Bowman Ratio II spectrometer equipped with a 150-W xenon light source and a Hamamatsu R928P photomultiplier tube. Tryptophanyl emission at 360 nm was monitored upon excitation at 295 nm. Fluorescence spectra and titrations were corrected for incident scatter and dilution as the result of added titrant. Inner filter effects due to acrylamide absorption were accounted for by the relationship $F_{corr} = F_{obs}10^{OD_{295}/2}$ where F_{obs} and F_{corr} denote the observed and corrected fluorescence intensities, respectively. OD_{295}, the absorbance by acrylamide, was calculated from the concentration and the extinction coefficient of 0.23 M^{-1} cm^{-1} (Eftink & Ghiron, 1976).

Nanosecond lifetime and polarization studies were carried out on a time-correlated fluorescence lifetime spectrometer from Photochemical Research Associates (London, Ontario, Canada) equipped with a J-Y monochromator on the excitation side and Glan-Thomson polarizers. Tryptophanyl fluorescence emission, upon excitation at 295 nm, was monitored through a Schott KV370 cutoff filter. Lifetimes were obtained with vertically polarized excitation and the emission polarizer set at the "magic angle" of 54.7°. In a typical experiment, 3 decades of intensity were accumulated. For anisotropy measurements, the vertically and horizontally polarized components of the fluorescence emission were monitored through a WG345 filter upon excitation at a wavelength of 300 nm. The channel density was 0.119 ns/channel. Lifetime measurements were conducted at room temperature; anisotropy measurements were conducted with the sample temperature maintained at 15.0 °C. Decay parameters were obtained by using the least-squares deconvolution method described by Grinvald and Steinberg (1974). Background scatter was accounted for by measuring aqueous solutions containing all components except protein. Lamp profiles were obtained by measuring excitation scatter from a dilute solution of glycogen.

In all cases, the protein was present in a 0.01 M Tris-HCl buffer, pH 7.4, in the absence and presence of the indicated inorganic salts. MBP concentrations were determined spectrophotometrically using $\epsilon^{1\%}_{276nm} = 5.89$ (Eylar & Thompson, 1969). Tryptophanyl quantum yields were obtained, as described by Chen (1972), relative to a value of 0.15 for NATA (Robbins et al., 1980).

Nanosecond Polarization Spectroscopy. The decay of fluorescence intensity is described by

$$I(t) = \sum f_i \exp(-t/\tau_i) \quad (1)$$

where f_i and τ_i denote the preexponential factor and lifetime of each component, respectively. When the fluorescence decay was nonexponential, the average lifetime $\langle\tau\rangle$, was obtained as $\langle\tau\rangle = \sum\alpha\tau_i/\sum\alpha_i$.

Time-dependent decay of anisotropy, $A(t)$, is given by

$$A(t) = [I_{VV}(t) - GI_{VH}(t)]/[I_{VV}(t) + 2GI_{VH}(t)] = D(t)/S(t) \quad (2)$$

where $I_{VV}(t)$ and $I_{VH}(t)$ represent the time dependence of the vertically and horizontally polarized intensities, respectively, the numerator represents the *difference*, $D(t)$, and the denominator the *sum*, $S(t)$, of the composite decay rates. For the case where depolarization occurs on a time scale comparable with the emission lifetime but within the duration of the excitation lamp profile, the difference between $I_{VV}(t)$ and $I_{VH}(t)$ can be quite small and comparable to the absolute

intensity, leading in turn to large uncertainties in the difference function $D(t)$. Such uncertainties in $D(t)$ are magnified by the presence of any polarization anomalies due to scatter from the face of the cuvette or the photomultiplier tube (Chen & Bowman, 1965). To account for any unequal transmission of polarized intensity, $I_{VH}(t)$ was multiplied by the ratio I_{HV}/I_{HH} determined in a separate measurement. This ratio is formally analogous to the G factor described for the unequal transmission of vertically and horizontally polarized light by diffraction grating monochromators (Azumi & McGlynn, 1962). In our case, a typical value for G was 1.05–1.12. $S(t)$ is analogous to the decay of the total fluorescence intensity and decays with a lifetime τ; the sum function can therefore be expressed in a manner analogous to eq 1, where $S(t) = S_0\sum \exp(-t/\tau)$, and S_0 denotes the initial intensity prior to emission.

The anisotropy decay rates were obtained in two ways. In the first method, $S(t)$ was deconvolved to obtain lifetimes and amplitudes. Employing these lifetimes and amplitudes from $S(t)$, we obtained decay parameters for $A(t)$ from eq 3

$$D(t) = S(t)A(t) \tag{3}$$

by minimizing the difference between the observed and fitted $D(t)$. This method has the advantage in that it minimizes $D(t)$, the data with the greatest uncertainty, and is therefore formally analogous to the treatment presented by Ross et al. (1981).

In a separate procedure, $D(t)$ and $S(t)$ were deconvoluted individually to obtain amplitudes and lifetimes that upon reconvolution with the experimental lamp function and combination would afford the anisotropy function. $A(t)$ determined in this manner was then compared by visual inspection with the observed $A(t)$ calculated by using eq 2 (Yguerabide, 1972). Both procedures afforded anisotropy decay profiles that were coincident.

For a rigid, spherical particle of volume V, $A(t)$ can be described by

$$A(t) = A_0 \exp(-t/\phi) = A_0 \exp(-6Dt) \tag{4}$$

where ϕ, the rotational correlation time (seconds), and D, the rotational diffusion coefficient (s^{-1}), are related to each other and to the volume of the macromolecule by eq 5, where V

$$\phi = 1/6D = \eta V/kT \tag{5}$$

(cm^3) is the hydrated volume of the protein particle, η (poise) is the viscosity, and k (erg deg^{-1} $molecule^{-1}$) is Boltzmann's constant.

Nonexponential decay of anisotropy, due either to nonspherical symmetry or to the intrinsic segmental flexibility of the particle, can be analyzed as a sum of two exponentials (Yguerabide, 1972). The following equation resolves the nonexponential decay into two major modes of rotational diffusion characterized by short (ϕ_S) and long (ϕ_L) correlation times and their corresponding amplitudes (f_S, f_L):

$$A(t) = A_0[f_S \exp(-t/\phi_S) + f_L \exp(-t/\phi_L)] \tag{6}$$

Bimolecular Quenching of Fluorescence. Energy transfer through bimolecular quenching can be analyzed by using the Stern–Volmer relationship where F and τ denote the fluorescence intensity and lifetime, respectively, and the subscript refers to the case denoting the presence of quencher, Q (eq 7). K_{SV} (M^{-1}) is the Stern–Volmer quenching constant.

$$F/F_Q = \tau/\tau_Q = 1 + K_{SV}[Q] \tag{7}$$

For dynamic quenching, a plot of F/F_Q, or τ/τ_Q, versus [Q] is predicted to be linear with a slope equal to K_{SV} and a y intercept of 1.0. The equilibrium quenching constant and the fluorescence lifetime are related to each other and to the bimolecular quenching constant k_q (M^{-1} s^{-1}) through the relationship $K_{SV} = k_q\tau$. The bimolecular quenching constant, a reflection of the encounter frequency between a fluorophore and Q, is proportional to temperature and inversely proportional to the viscosity of the bulk medium.

Deviation of Stern–Volmer plots from linearity is indicative of the presence of static quenching, an additional mode of energy transfer that serves to cause a reduction in fluoresence intensity without a corresponding reduction in fluorescence lifetime. When both dynamic and static quenching mechanisms are present, the Stern–Volmer equation can be described by eq 8 where K_{SV} and K_S denote the dynamic and static

$$F/F_Q = (1 + K_{SV}[Q])(1 + K_S[Q]) \tag{8}$$

quenching constants, respectively. In an alternative treatment (eq 9), the presence of static quenching is accounted for

$$F/F_Q = (1 + K_{SV}[Q]) \exp(V[Q]) \tag{9}$$

through a constant, V (M^{-1}), that represents the volume of a "sphere of action" in which the quencher and fluorophore coexist at the moment of excitation. In the case of acrylamide quenching of tryptophanyl fluorescence, the upward curvature has been effectively analyzed by using eq 9 (Lehrer & Leavis, 1978; Eftink & Ghiron, 1981). It is noteworthy that as $V \rightarrow 0$, the term $\exp(V[Q])$ approaches $1 + V[Q]$, and eq 9 becomes formally analogous to eq 8, which is to say that $V \rightarrow K_S$.

Results

Influence of Ionic Composition on Myelin Basic Protein Tryptophanyl Fluorescence. The uncorrected fluorescence emission spectrum of MBP appeared with a maximum at 363 nm (λ_{corr} = 346 nm) upon excitation at 295 nm and was characterized by a quantum efficiency of 0.04. The tryptophanyl fluorescence intensity of MBP increased in a near-linear manner with increasing concentration over the range 0–2.0 M NaCl (Figure 1); there was no evidence of saturation. In the presence of 1.0 M NaCl, MBP fluorescence increased approximately 22%, while in the presence of 2.0 M NaCl the increase was 46%. These increases were accompanied by blue-shifts in the emission spectrum of 2 and 5 nm, respectively. The fluorescence decay of MBP was adequately described by a two-exponential equation (χ^2 = 1.2) containing lifetimes of 1.99 ± 0.02 and 4.13 ± 0.05 ns present in a respective ratio of preexponential factors of 4 to 1 ($\langle\tau\rangle$ = 2.44 ± 0.02 ns). The increased fluorescence was due to increases in both the short- and long-lifetime components without change in the respective preexponential factors. As shown in the inset of Figure 1, the average lifetime increased in a manner that paralleled the increases in steady-state fluorescence.

The dependence of MBP tryptophanyl fluorescence on the ionic composition of the medium was examined further with respect to mono- and divalent chloride salts (KCl, LiCl, $CaCl_2$, and $MgCl_2$) and a series of polyvalent sodium salts ($NaClO_4$, Na_2SO_4, and Na_3PO_4). In all cases, fluorescence intensity increased with increasing concentrations of added electrolyte. There was no evidence of saturation. When analyzed with respect to ionic strength (Figure 2), MBP fluorescence increased to the same magnitude in the presence of mono- and divalent salts. With the exception of results for ClO_4^-, which was shallower than for the other electrolytes, all titration profiles were essentially congruent. In the presence of both NaCl and $CaCl_2$, the tryptophanyl fluorescence intensity of MBP was the additive sum of the intensities measured in the presence of the individual salts alone (data not shown). Similar behavior was observed for NaCl in the presence of $MgCl_2$. Overall, it was noteworthy that the effects of the ionic salts

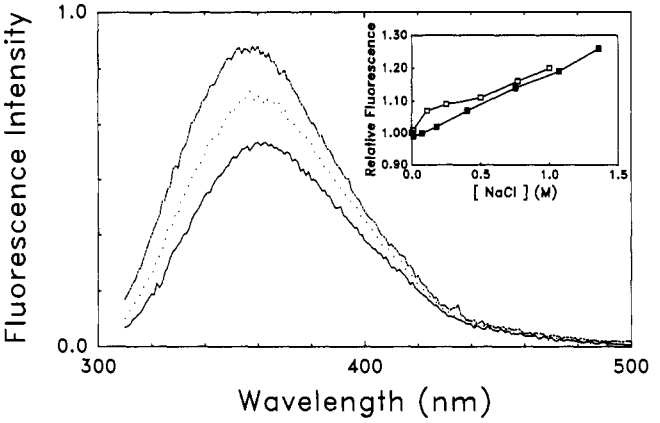

FIGURE 1: Dependence of myelin basic protein fluorescence on the concentration of NaCl. Steady-state fluorescence spectra of MBP in the absence (—) and presence of increasing concentrations of NaCl [(···) 1.0 M; (- - - -) 2.0 M]. Inset: Intensities at 360 nm were measured upon excitation at 295 nm in the presence of the indicated concentrations of NaCl (■). MBP was present at a concentration of (1–2) × 10^{-6} M in 0.01 M Tris-HCl buffer, pH 7.4, in the absence of NaCl. Similar results obtained with respect to the average lifetime, $\langle\tau\rangle$, are also presented (□). The quantity $\langle\tau\rangle$ was the weighted average of two components, τ_1 of 2.01 ns, which increased 10%, and τ_2 of 4.03 ns, which increased 20%. The corresponding amplitudes, α_1 and α_2, were invariant with NaCl concentration. For lifetime measurements, MBP was present at concentrations of (25–30) × 10^{-6} M. Emission decay profiles were obtained through a KV370 Schott cutoff filter upon excitation at 295 nm.

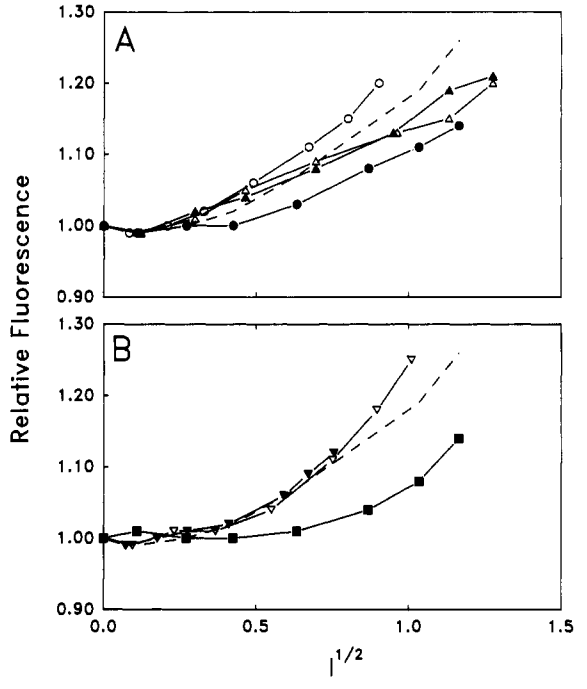

FIGURE 2: Influence of the ionic strength of mono- and divalent electrolyte solutions on the intrinsic fluorescence of myelin basic protein. Steady-state fluorescence intensity of MBP (λ_{ex} = 295 nm; λ_{em} = 360 nm) was measured in 0.01 M Tris-HCl buffer, pH 7.4, in the presence of the indicated salts. MBP was present at a concentration of (1–2) × 10^{-6} M. (Panel A) (△) $CaCl_2$; (▲), $MgCl_2$; (○) KCl; (●) LiCl. (Panel B) (▼) Na_3PO_4; (▽) Na_2SO_4; (■) $NaClO_4$. The dashed line indicates the results obtained for NaCl. Changes in fluorescence are plotted against the square root of the ionic strength, $I^{1/2}$, where $I = (1/2)\sum c_i z_i^2$.

on MBP fluorescence were attributable to contributions from both the cationic and the anionic species.

As a frame of reference, the spectral characteristics of MBP were compared with those for HSA and NATA. The emission maximum for NATA (λ_{corr} = 350 nm) was similar to that for

Table I: Equilibrium and Bimolecular Constants for Quenching by Acrylamide of Myelin Basic Protein, Human Serum Albumin, and *N*-Acetyltryptophanamide in the Absence and Presence of NaCl[a]

[NaCl] (M)	[protein] (μM)	K_{SV}^{SS} (M^{-1})	V (M^{-1})	K_{SV}^{τ} (M^{-1})	$k_q \times 10^{-9}$ (M^{-1} s^{-1})
		Myelin Basic Protein			
0	1	15.7 ± 0.4	1.1 ± 0.1		
	25–50	8.9 ± 0.2	1.1 ± 0.1	7.4 ± 0.2	3.0 ± 0.1[b]
1.0	1	13.6 ± 0.4	0.9 ± 0.1		
	25	11.1 ± 0.5	1.7 ± 0.2	7.0 ± 0.4	2.4 ± 0.2[b]
		Human Serum Albumin			
0	1	6.6 ± 0.4	0.7 ± 0.1		
	25–50	5.0 ± 0.3	1.0 ± 0.1	3.7 ± 0.3	1.1 ± 0.1[c]
1.0	1	8.2 ± 0.5	0.5 ± 0.1		
	25–50			6.0 ± 1.4	1.6 ± 0.3[c]
		N-Acetyltryptophanamide			
0	1.0	18.8 ± 0.5	3.0 ± 0.2		
	30–100			16.0 ± 0.5	5.6 ± 0.2
1.0	10	18.2 ± 0.9	1.7 ± 0.2		
	30–100			16.4 ± 0.6	5.6 ± 0.01

[a] All values reported represent the mean ± SEM averaged over at least two independent determinations. K_{SV}^{SS} and K_{SV}^{τ} denote equilibrium quenching constants determined from steady-state measurements and fluorescence lifetime values, respectively. [b] Bimolecular quenching constants, k_q, were calculated from knowledge of K_{SV}^{τ} and the average lifetime $\langle\tau\rangle$. [c] Bimolecular quenching constants were calculated from knowledge of K_{SV} and τ_1, the shorter of the two lifetime components. The longer component, τ_2, underwent neither dynamic nor static quenching.

MBP, but was considerably red-shifted with respect to the emission maximum of HSA (λ_{corr} = 337 nm), which was characterized by a quantum efficiency of 0.10. NATA fluorescence decayed with a single emission component with a lifetime of 2.87 ± 0.02 ns. Fluorescence decay of HSA was described by a two-exponential equation (χ^2 = 1.5) from which the lifetimes were derived to be 3.39 ± 0.09 and 7.53 ± 0.06 ns present in a ratio of preexponential factors of 0.45 to 0.55. The average lifetime of 5.66 ± 0.01 ns for HSA when compared with the average lifetime of 2.44 ± 0.02 ns for MBP was in excellent agreement with the ratio of steady-state quantum yields. In contrast to the case for MBP, the fluorescence intensity and lifetimes of HSA and NATA were unchanged in the presence of 1.0 M NaCl.

Bimolecular Quenching of Myelin Basic Protein Tryptophanyl Fluorescence. The accessibility of the tryptophanyl residue in MBP to the medium was assessed by measuring the capacity for acrylamide quenching of the intrinsic protein fluorescence. Stern–Volmer plots derived from measurement of the steady-state fluorescence for MBP deviated from linearity and showed marked upward curvature over the acrylamide concentration range 0–0.3 M (not shown). This behavior was more pronounced for MBP than for HSA, but less pronounced than for NATA. Such nonlinear behavior was indicative of the presence of both dynamic and static components to quenching, and could be analyzed by using eq 9 to obtain values for the dynamic and static quenching constants, K_{SV} and V, respectively (Table I). The equilibrium quenching constants for MBP and NATA, 15.7 ± 0.4 and 18.8 ± 0.5 M^{-1}, respectively, were comparable but more than 2-fold greater than for quenching of HSA (6.6 ± 0.4 M^{-1}). At MBP concentrations of 50 μM, K_{SV} was calculated to be 8.9 ± 0.2 M^{-1}, signifying a small but measurable dependence of bimolecular quenching on protein concentration. Such a dependence of quenching on protein concentration was not observed for HSA. In all cases, values for the static quenching constant, V, derived from analysis of eq 9, were in the range 0–3.0 M^{-1} and were invariant with protein concentration (Table I).

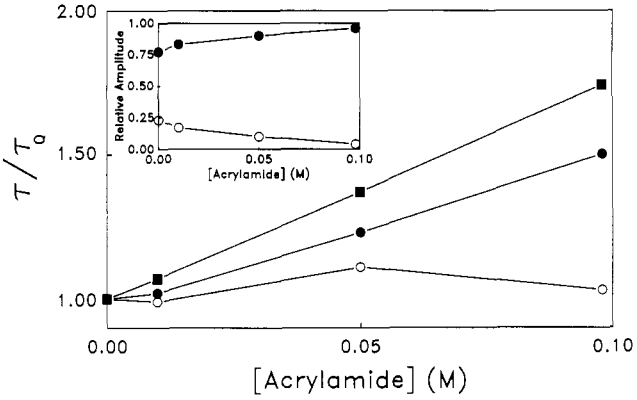

FIGURE 3: Stern–Volmer plots for myelin basic protein derived from measurement of lifetime decay rates. τ_1/τ_0 increased in the presence of increasing concentrations of acrylamide while τ_2/τ_0 was essentially invariant with acrylamide concentration. From the slopes of the Stern–Volmer plots, K_{SV} calculated from τ_1 (●), τ_2 (○), and $\langle\tau\rangle$ (■) was determined to be 5.2, 0.5, and 7.6 M^{-1}, respectively, averaged over three determinations, K_{SV} for τ_1, τ_2, and $\langle\tau\rangle$ was calculated to be 5.1 ± 0.1, 0.2 ± 0.2, and 7.4 ■ 0.2 M^{-1}, respectively. Inset: The relative amplitude of τ_1 increased and that for τ_2 decreased with increasing acrylamide concentration.

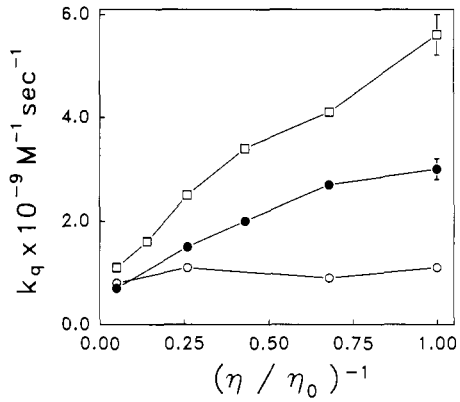

FIGURE 4: Dependence of the bimolecular quenching constant on the viscosity of the bulk aqueous medium. Fluorescence lifetimes of MBP, HSA, and NATA, present at concentrations of (50–100) × 10^{-6} M in 0.01 M Tris-HCl buffer, pH 7.4, were measured at 23 °C as a function of acrylamide concentration in the presence of different amounts of glycerol (0–80%, w/v). Bimolecular acrylamide quenching constants, k_q (M^{-1} s^{-1}), for MBP (●), HSA (○), and NATA (□), were obtained by using K_{SV} (M^{-1}) = τ (s)k_q. Quenching constants K_{SV} were derived from the slopes of τ/τ_0 versus [Q] plots. Data are presented as k_q versus the reciprocal of the relative viscosity. k_q for MBP was calculated by using the average lifetime while for HSA the short dynamically quenched lifetime component τ_1 was used.

Each of the two lifetime components determined for MBP underwent quenching in a linear manner with acrylamide concentration and obeyed the Stern–Volmer relationship for dynamic quenching (eq 7). Quenching of τ_1 exceeded that of τ_2 (Figure 3). The preexponential factor for the τ_2 component decreased sharply with increasingly acrylamide concentrations, and in the presence of 0.1 M acrylamide represented less than 5% of the total amplitude. From the slope of the Stern–Volmer plot constructed from values of τ_1, K_{SV} was calculated to be 5.1 ± 0.1 M^{-1}. For the second component, τ_2, the value of K_{SV} was calculated to be 0.2 ± 0.2 M^{-1}, the large error in K_{SV} for τ_2 was attributed to the uncertainty engendered in measuring a component present in less than 5% of the total amplitude. On the basis of the average lifetime, $\langle\tau\rangle$, K_{SV} was calculated to be 7.4 ± 0.2 M^{-1} (Table I). Dynamic quenching constants calculated from steady-state and emission decay kinetics were in close agreement when determined at equivalent concentrations of MBP (Table I). Hence, the data indicated that quenching of τ_2 occurred principally through static mechanisms, attributable to a ground-state phenomenon without alteration in lifetime, whereas the short-lifetime component τ_1 underwent dynamic quenching, an excited-state phenomenon attributable to a reduction in lifetime.

Steady-state and time-resolved acrylamide quenching of a given concentration of MBP was identical in the presence and absence of 1.0 M NaCl (Table I). In the presence of 1.0 M NaCl, and at an MBP concentration of 1.0 μM, K_{SV} determined through steady-state techniques was calculated to be 13.6 ± 0.4 M^{-1}, not remarkably different from those observed in the absence of NaCl. Similarly, K_{SV} determined through lifetime quenching was calculated based on values of $\langle\tau\rangle$ to be 7.0 ± 0.4 M^{-1}, not remarkably different from those observed in the absence of NaCl.

Bimolecular quenching of HSA or of NATA was not remarkably different in the absence and presence of NaCl (Table I). the quenching constant for HSA derived from analysis of τ_1 was calculated to be 3.7 ± 0.3 M^{-1}, the amplitude and lifetime of the longer component, τ_2, remained unchanged up to 0.15 M acrylamide, and therefore underwent neither dynamic nor static quenching. For NATA, the quenching constant derived from the single lifetime was calculated to be 16.0 ± 0.5 M^{-1}. For both HSA and NATA, the quenching constants derived from steady-state and lifetime measurements were in good agreement.

Dependence of Bimolecular Quenching on the Viscosity of the Bulk Medium. The acrylamide bimolecular quenching constant, k_q, was determined as a function of the bulk viscosity. Emission decay rates of MBP were measured as a function of acrylamide concentration in the presence of increasing concentrations of glycerol in the range 0–80% (w/v), corresponding to relative viscosities of 1–25. Values for k_q, based on values of the average lifetime, $\langle\tau\rangle$, and K_{SV} derived from $\langle\tau\rangle$, versus the inverse viscosity determined at different concentrations of glycerol are presented in Figure 4. The bimolecular quenching rate constant of MBP fluorescence approached the diffusion limitation, exceeding 1 × 10^9 M^{-1} s^{-1}, and showed a near-linear dependence on the viscosity of the bulk aqueous medium.

In contrast to the case for MBP, k_q for HSA was essentially independent of viscosity, and displayed a near-constant value of approximately 1.0 × 10^9 M^{-1} s^{-1}. The quenching rate for NATA showed the steepest dependence on the viscosity of the medium. At high concentrations of glycerol, k_q for MBP, HSA, and NATA converged at a common value of approximately 1 × 10^9 M^{-1} s^{-1}.

Anisotropy Decay of Myelin Basic Protein. Local flexibility and overall mobility of MBP were assessed by determining the time-dependent polarization decay of tryptophanyl fluorescence. There was observed only a small difference between the time-dependent decay of $I_{VV}(t)$ and $I_{VH}(t)G$ at peak intensity, and the polarized components became coincident within 2 ns of the peak intensities (Figure 5A, inset). The experimental anisotropy decay was adequately described by a single-exponential equation characterized by a correlation time of 1.0 ± 0.08 ns and a limiting anisotropy of 0.118 ± 0.005 (Figure 5B). This correlation time was in excellent agreement with the longer of the two correlation times (0.09 and 1.26 ns) obtained by Munro et al. (1979) employing synchrotron excitation, but was markedly lower than the value of 7.4 ns predicted on the basis of a rigid sphere of 18.5K molecular weight. The limiting anisotropy of 0.12 was approximately half that of 0.256 reported by other investigators (Munro et al., 1979; Lakowicz et al., 1983).

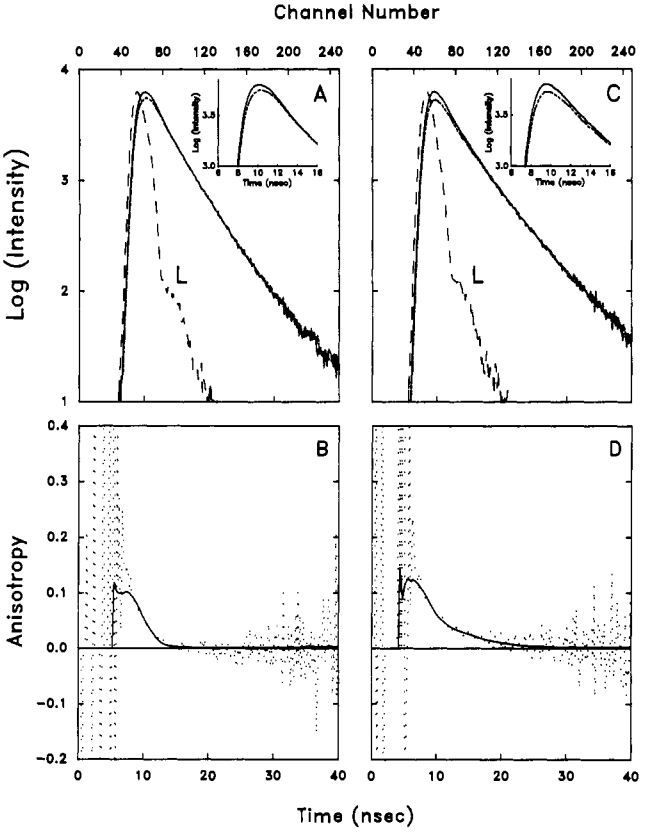

FIGURE 5: Anisotropy decay of myelin basic protein in the absence and presence of NaCl. Time-dependent decays for the component-polarized intensities and experimental and fitted anisotropy decay profiles were measured and calculated as described under Materials and Methods. Myelin basic protein was present at concentrations in the range (50–100) × 10^{-6} M in 0.01 M Tris-HCl buffer, pH 7.4, in the absence and presence of 1.0 M NaCl. Panel A shows the time-dependent decay of $I_{VV}(t)$ (—) and $I_{VH}(t)G$ (- - -) along with the lamp profile (L). The G factor for the profile shown was 1.12. At the peak intensities, there was a measurable difference between $I_{VV}(t)$ and $I_{VH}(t)$ which became coincident within 2 ns of the peak intensity (inset). Panel B shows the experimental (···) and fitted (—) anisotropy decays calculated from the data in panel A. The anisotropy decayed to zero and was described by a single-exponential equation with a rotational correlation time of 0.99 ns and r_0 of 0.127. Averaged over four separate determinations, the correlation time was 1.01 ± 0.08 ns, and r_0 was 0.118 ● 0.005. Panel C shows the anisotropy decay for MBP determined in 0.01 M Tris-HCl buffer, pH 7.4, containing 1.0 M NaCl. In this case, the difference between $I_{VV}(t)$ (—) and $I_{VH}(t)G$ (- - -) at the peak intensities was greater and required 6 ns to become coincident (inset) compared to the case in panel A for the absence of NaCl. Panel D shows the experimental (···) and fitted (—) anisotropy decays calculated from the data in panel C. The anisotropy decayed to zero but, in contrast to the data in panel B, was not adequately described by a single-exponential equation. Analysis of $A(t)$ afforded two components with correlation times of 0.59 and 6.3 ns and r_0 of 0.16. Average over four determinations, correlation times of 0.65 ± 0.13 and 9.1 ± 1.8 ns and r_0 of 0.16 ± 0.01 were observed.

In solutions of 0–0.3 M NaCl, fluorescence depolarization of MBP continued to obey exponential behavior but slowed from 1.0 to 1.6 ns (Table II). In the presence of 0.5–1.0 M NaCl, the difference between $I_{VV}(t)$ and $I_{VH}(t)G$ was measurably greater than when determined in the absence of salt, and the polarized components required 6 ns from peak intensity to reach coincidence (Figure 5C, inset). The anisotropy decay of MBP in the presence of 0.5–1.0 M NaCl deviated from exponential behavior and required analysis with an equation containing a sum of two exponential terms (Figure 5D, Table II). In the presence of 1.0 M NaCl, correlation times of 0.65 ± 0.13 and 9.1 ± 1.8 ns and a limiting anisotropy of 0.16 ± 0.01 were obtained. The limiting anisotropy of 0.16 was comparable with that seen in the absence of NaCl. The slower component of depolarization and the nonexponential behavior were evident also in solutions of LiCl (1.0 M), $MgCl_2$ (0.5 M), and $CaCl_2$ (0.5 M). For HSA, the presence of NaCl caused no discernible alteration in shape or magnitude of the anisotropy decay profile (Table II).

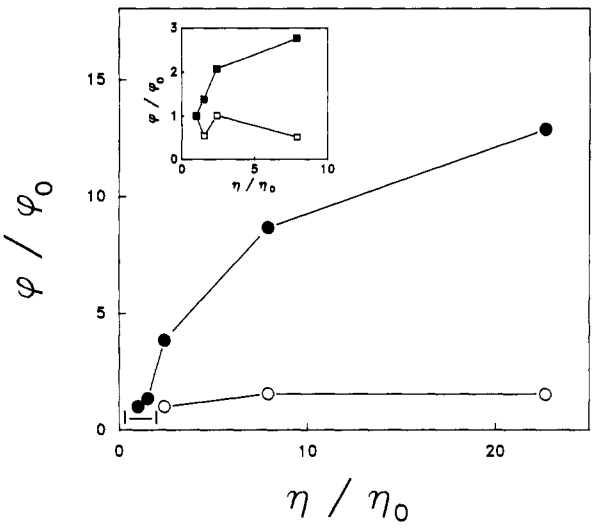

FIGURE 6: Dependence of rotational correlation time of myelin basic protein on the viscosity of the bulk aqueous medium. Time-correlated depolarization decay times were obtained at 15 °C for MBP in 0.01 M Tris-HCl buffer, pH 7.4, containing different amounts of glycerol (0–80% w/v). MBP was present at a concentration of 50 × 10^{-6} M. Short (○) and long (●) rotational correlation times of MBP were determined in the absence (ϕ_0) and presence (ϕ) of increasing concentrations of glycerol, and are presented as the ratio of the correlation times (ϕ/ϕ_0) versus the relative viscosity (η/η_0). Below glycerol concentrations of 30% (η/η_0 = 2.42), only a single correlation time was observed (denoted by the bar). This correlation time increased 9-fold in a near-linear fashion with increasing amounts of glycerol up to 60% glycerol (η/η_0 = 7.9). At higher concentrations of glycerol, a second component having a correlation time of 0.3–0.6 ns was evident. This component was essentially invariant with increasing viscosity. When both components were observed, r_0 was 0.20–0.22. When only the slower component was evident, r_0 was approximately 0.10. Inset: Similar data obtained for rotational depolarization of HSA as a function of glycerol concentration. The long correlation time (■) increased 3-fold in a near-linear fashion up to a glycerol concentration of 30%. The short correlation time (□) was invariant with increasing glycerol concentrations and had a value of 0.4–0.6 ns.

Dependence of the Anisotropy Decay on the Viscosity of the Bulk Medium. In order to resolve rapid components of depolarization, anisotropy measurements of MBP were conducted as a function of the viscosity of the bulk aqueous medium in the presence of different concentrations of glycerol (Figure 6). The 1-ns correlation time increased in a near-linear fashion with increasing glycerol concentration up to 60% (w/v) glycerol (η/η_0 = 7.9). At glycerol concentrations greater than 30%, corresponding to relative viscosities greater than 2.4, a subnanosecond component of 0.3–0.6 ns was evident. When the relative viscosities of 2.4 for 30% and 7.9 for 60% (w/v) glycerol were taken into account, this component was characterized by a correlation time of 0.07–0.14 ns and an amplitude of 0.13–0.14. Identical results were obtained when measured in the presence of comparable solutions of sucrose. Overall, the anisotropy decay characteristics of MBP in the presence of either glycerol or sucrose were comparable to the results obtained by using fast-excitation energy sources in the absence of viscosimetric agents (Munro et al., 1979).

The anisotropy decay for HSA was described by a sum of two exponential terms with correlation times of 0.55 ± 0.08

Table II: Rotational Correlation times and Limiting Anisotropies for Myelin Basic Protein and Human Serum Albumin in the Absence and Presence of Mono- and Divalent Electrolytes[a]

salt	[salt] (M)	f_s	ϕ_1 (ns)	f_L	ϕ_2 (ns)	r_0
			Myelin Basic Protein			
NaCl	0	0.118 ± 0.005	1.01 ± 0.08			0.118 ± 0.005
	0.1	0.113 ± 0.001	1.45 ± 0.14			0.113 ± 0.001
	0.3	0.108 ± 0.002	1.61 ± 0.08			0.108 ± 0.002
	0.5	0.107 ± 0.006	0.43 ± 0.02	0.053 ± 0.002	4.7 ± 0.2	0.160 ± 0.006
	1.0	0.098 ± 0.006	0.65 ± 0.13	0.064 ± 0.004	9.1 ± 1.8	0.16 ± 0.01
LiCl	1.0	0.15 ± 0.02	0.24 ± 0.08	0.061 ± 0.005	4.1 ± 0.8	0.21 ± 0.02
$CaCl_2$	0.5	0.12 ± 0.01	0.48 ± 0.11	0.045 ± 0.004	7.1 ± 1.2	0.17 ± 0.01
$MgCl_2$	0.5	0.128 ± 0.002	0.37 ± 0.04	0.061 ± 0.005	6.5 ± 0.95	0.19 ± 0.01
			Human Serum Albumin			
NaCl	0	0.061 ± 0.008	0.55 ± 0.08	0.133 ± 0.006	36.5 ± 1.4	0.19 ± 0.01
	1.0	0.066 ± 0.006	0.63 ± 0.13	0.14 ± 0.01	50.2 ± 0.9	0.21 ± 0.02

[a] Reported Values represent the mean ± SEM averaged over at least two independent determinations.

and 36.5 ± 1.4 ns and a value for r_0 of 0.19 ± 0.01. In glycerol-containing solutions, the long correlation time of HSA increased with increasing glycerol concentration while the subnanosecond correlation remained unchanged over the whole range. Whereas the correlation times for MBP increased nearly 8-fold in the presence of 60% glycerol, that for HSA increased more modestly, from 37 to 100 ns, i.e., approximately 3-fold, under the same conditions (Figure 6, inset). That is, fluorescence depolarization of MBP was far more sensitive to the presence of glycerol than was that of HSA.

Discussion

Influence of Electrolytes on the Intrinsic Tryptophanyl Fluorescence of Myelin Basic Protein. Trp-115, the single tryptophanyl residue of MBP, is characterized by a red-shifted fluorescence emission spectrum (λ_{corr} = 346 nm), a low quantum yield (0.04), and a short fluorescence lifetime ($\langle\tau\rangle$ = 2.44 ns), spectral characteristics that closely resemble those observed for NATA and other tryptophanyl analogues in aqueous solution. Acrylamide quenching of Trp-115 of MBP is rapid ($>10^9$ M^{-1} s^{-1}), occurring at rates approaching the diffusion limitation and comparable with those measured for HSA and NATA, and therefore provides no basis for discriminating physical differences in the respective tryptophanyl environments. The invariance of bimolecular quenching of HSA fluorescence with viscosity indicates that direct encounter between acrylamide and the tryptophanyl residue is not diffusion-limiting but instead requires permeation of the acrylamide through the protein matrix (Eftink & Hagaman, 1986). This behavior is consistent with the single tryptophanyl residue of HSA residing within the protein matrix and therefore occluded from contact with the bulk aqueous medium. For MBP and NATA, however, the marked dependence of bimolecular quenching on viscosity is indicative of a diffusion-limited encounter between acrylamide and Trp-115, leading in turn to the conclusion that Trp-115 is readily exposed to the bulk aqueous medium.

The salient finding of this study reveals that the fluorescence of Trp-115 in MBP is measurably dependent on the ionic composition of the bulk aqueous medium. Steady-state fluorescence and fluorescence lifetimes of Trp-115 increase in a near-linear manner with increasing concentrations of mono- and divalent electrolytes. The increase in fluorescence is attributable to the combined effect of the cationic and anionic species, occurs without any substantial alteration in the rate of bimolecular quenching, and closely parallels the ionic strength of the bulk aqueous medium.

Two limiting mechanisms through which an electrolyte-induced change in the Trp-115 fluorescence can arise are shown in Figure 7. *Mechanism A* proposes that the fluorescence of MBP is governed by exposure of Trp-115 to the bulk aqueous medium and that the presence of electrolytes alters the spatial relationship between Trp-115 and the bulk aqueous medium. In the presence of electrolytes, Trp-115 is removed from the protein surface to within an occluded nonpolar region of the protein. This case predicts a blue-shift in the tryptophanyl emission spectrum and a decrease in accessibility of the residue to the bulk aqueous medium in the presence of added electrolyte. *Mechanism B* proposes that the intrinsic fluorescence of MBP is governed by intramolecular quenching through the proximity of Trp-115 with a neighboring amino acid residue that quenches tryptophanyl fluorescence; the essential feature of this case is that the presence of electrolytes alters the spatial relationship between Trp-115 and a neighboring amino acid residue of the protein and, therefore, the extent of intramolecular quenching. This case predicts an increase in fluorescence without alteration in spectral position and without a corresponding alteration in tryptophanyl accessibility to the

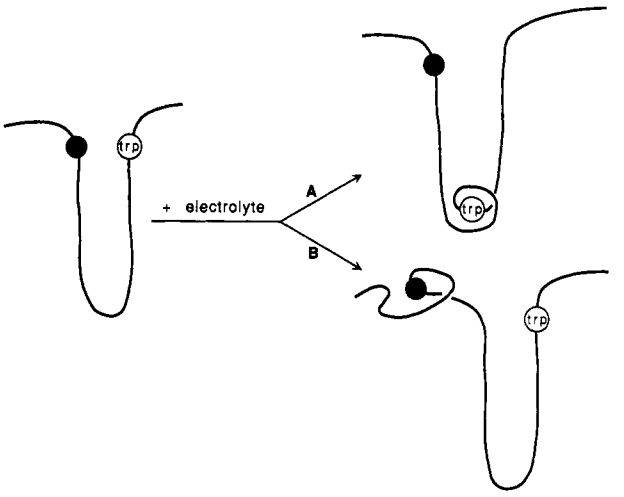

FIGURE 7: Model explanations for the influence of electrolytes on the conformation of MBP in solution. The influence of ionic strength on the fluorescence of Trp-115 of MBP is viewed as arising through either of two distinct mechanisms. A segment of MBP containing Trp-115 is depicted. In *mechanism A*, the presence of added electrolyte serves to alter the protein conformation such that Trp-115 becomes buried within a nonpolar cavity of the protein and experiences a decrease in accessibility to the bulk aqueous medium. In this case, the change in fluorescence reflects a change in the polarity of the immediate local environment. *Mechanism B* proposes that Trp-115 is in neighboring proximity with a specific amino acid residue (●) that quenches the intrinsic fluorescence. In this case, the presence of added electrolytes removes the quenching residue from proximity with Trp-115, and the change in fluorescence arises from a relief of intramolecular quenching.

bulk medium. While not mutually exclusive, both mechanisms require a change in the solution conformation of MBP.

Emission spectra for MBP in the presence of 1–2 M NaCl undergo a blue-shift of 2–5 nm, from 363 to 358 nm, implicating a modest change in polarity of the immediate tryptophanyl environment. The final position of 358 nm, however, remains well-removed from the 351-nm emission maximum characteristic of HSA, for which independent evidence indicates occlusion of the tryptophanyl residue from the bulk medium. The dynamic and static bimolecular quenching rate constants for MBP are unchanged in the presence and absence of NaCl, indicating no discernible decrease in accessibility to the bulk aqueous medium. These findings argue against mechanism A. The increase in fluorescence lifetimes of MBP with increasing concentrations of NaCl is indicative of a *reduction* in the extent of dynamic quenching. This behavior closely resembles that seen for changes in the fluorescence spectra, quantum yields, and lifetimes upon immersion of MBP in the denaturant urea, suggesting that the changes are related to a change in protein conformation. Overall, the present results argue that electrolyte-induced changes in the intrinsic fluorescence of MBP are governed by relaxation of intramolecular quenching rather than by an alteration in polarity of the immediate environment. It has been demonstrated that tryptophan in aqueous solution can undergo fluorescence quenching through charge-transfer or proton-transfer interactions between the excited indole ring and quaternary ammonium groups (Shizuka et al., 1988). This suggests that a quaternary ammonium group of a lysine or arginine residue in proximity of Trp-115 could serve as a possible intramolecular quencher.

No distinctions are evident between the effects on MBP seen for mono- and divalent cations (Li^+, Na^+, K^+, Mg^{2+}, Ca^{2+}) and multivalent anions (Cl^-, SO_4^{2-}, PO_4^{3-}), species with differing charge/radius ratios. While the results for ClO_4^- are less steep than seen for the other electrolytes, solutions of perchlorate are notable for their nonideal behavior (Berman & Stengle, 1975a,b). In all cases, the salt-induced changes in MBP fluorescence are in the same direction and are proportional to electrolyte concentration; the titration profiles are essentially congruent and directly parallel the ionic strength of the bulk aqueous medium independent of the electrolyte valence (Figure 2). An explanation for these observations based solely on a direct ion binding mechanism would require ion association at specific residues and would be predicted to be saturable. Such a case has been observed for the influence of mono- and divalent electrolytes on the solution conformation of acetylcholinesterase, an enzyme that carries a high net negative charge (Nowak & Berman, 1991). Also, because of the high net positive charge carried by MBP, it is anticipated that anions would show preferential binding over cations and therefore exert greater effects. Yet, the electrolyte-induced changes in fluorescence are nearly equipotent irrespective of the valence and charge/radius ratio of the individual electrolyte species. The direct parallel between the intrinsic fluorescence and ionic strength of the medium implies that the solution conformation of MBP depends on shielding of its high net positive charge by the ionic medium.

Influence of Electrolytes on Rotational Depolarization of Myelin Basic Protein. Anisotropy decay rates for MBP ($\phi \leq 1$ ns) exceed those predicted for rotation of a rigid spherical volume of revolution ($\phi_{sphere} \approx 7$ ns). The correlation time of 0.07–0.14 ns, extrapolated on the basis of viscosity of the bulk medium, is comparable to the correlation time of 0.09 ns observed directly by synchrotron excitation (Munro et al., 1979), and is suggestive of a mode of depolarization that originates from rotation about a single bond either of the tryptophan moiety or of the indole side chain (McCammon & Harvey, 1987). It is significant that anisotropy decay of MBP, an 18.5-kDa species made up of 169 amino acids, occurs on a time scale that is rapid relative to macromolecular rotational diffusion, and is comparable with that observed for short polypeptides such as ACTH and glucagon which contain 24 and 37 amino acids, respectively (Chen et al., 1987). When compared with the muted viscosity dependence for fluorescence depolarization of HSA, which closely parallels that predicted for a rigid spherical particle of 66-kDa molecular mass, the behavior observed for MBP indicates unequivocally that Trp-115 is associated with a mobile segment of the protein (Munro et al., 1979).

The presence of electrolytes causes a concentration-dependent slowing of rotational depolarization of MBP. The effect is seen for MBP, but not for HSA, and is evident through the appearance of a 5–10-ns correlation time that accompanies the 1-ns component. This behavior is observed also in the presence of LiCl, $MgCl_2$, and $CaCl_2$, and hence occurs independent of the nature of the individual electrolytes. A reduction in the rate of fluorescence depolarization in the presence of electrolytes can reflect either a reduction in protein segmental flexibility or formation of higher protein aggregates.

A reduction in the segmental motion of MBP would be evident as a reduction in the amplitude of the fast (1 ns) component of decay and a corresponding increase in amplitude of the slow (5–10 ns) component. That is, such an explanation predicts a reciprocal relationship between amplitudes of the fast and slow components. The amplitude of the fast component, however, remains dominant at a near-constant percentage of the total observed amplitude, and is not markedly reduced with increasing electrolyte concentration (Table II). Since MBP in the presence of added electrolytes continues to display high segmental flexibility, the present results do not accommodate an electrolyte-induced reduction in segmental flexibility and therefore direct attention to the colligative behavior of MBP in solution. As assessed from sedimentation equilibria (Smith, 1980), circular dichroism (Smith, 1985; Gow & Smith, 1989), rapid kinetic techniques measuring light scattering (Young et al., 1982; Lampe et al., 1983), and equilibrium chromatography (Moskaitis et al., 1987), MBP is long known to undergo self-association. In all cases, the association is reported to be relatively weak and not detected at protein concentrations below 50 μM. The observation of a distinct component of anisotropy decay, in the range 5–10 ns, that is absent in the absence of electrolytes but can be resolved in the presence of electrolyte concentrations greater than 0.5 M (Figure 5C,D; Table II), is consistent with an electrolyte-induced self-association of MBP. In this condition, however, MPB appears to retain its intrinsic flexibility since the 0.5–1-ns decay component is explicitly evident on the time axis while the extrapolated 0.1-ns component is implicitly evident through a value of r_0 that is less than maximum.

These studies therefore reveal that electrolytes *promote* rather than diminish the capacity for MBP self-association. The phenomenon of self-association of MBP under conditions of higher rather than lower ionic strength is reminiscent of the case for nucleic acids and for protein–nucleic acid interactions, and is explained with respect to shielding of repulsive Coulombic interactions by the surrounding ionic medium (Record et al., 1978). In view of the high net charge carried by MBP, the increased propensity for self-association in the presence of electrolytes is likely attributable to ionic shielding

conferred by the bulk ionic medium.

Functional Significance of Myelin Basic Protein Flexibility. As mentioned at the outset, the structure of MBP and the physical determinants that govern its behavior in solution are not known. These studies, employing multiple independent spectroscopic indexes, reveal a dependence of MBP conformation and self-association on the ionic strength of the bulk aqueous medium. Since MBP is a cytoplasmic species, functionally linked alterations in the ionic composition of the cytoplasm, which may likely accompany wrapping and compaction of an oligodendrocyte or Schwann cell process around an axon, represent one signal worthy of consideration in assessing the role of MBP in mediating myelination.

It is anticipated that compaction of an oligodendrocyte or Schwann cell process results in a reduction in the cytoplasmic volume, leading in turn to relatively large increases in intracellular ion concentrations. The basal concentrations of Na^+, K^+, and Cl^- in cultured oligodendrocytes from mouse spinal cord are estimated to be 0.015, 0.070, and 0.007–0.030 M, respectively (Kettenmann et al., 1983; Kettenmann, 1987; Ballanyl & Kettenmann, 1990). A halving of the dimensions of the uncompact oligodendrocyte would lead to an 8-fold reduction of the intracellular volume and an 8-fold increase in the ion concentrations. In these cases then, the respective concentrations of Na^+, K^+, and Cl^- would rise to 0.125, 0.5, and 0.24 M in the compact process, concentrations comparable to those shown here to cause alterations in the solution behavior of MBP. Should myelin compaction engender alterations in ionic composition of the cytoplasm, then such alterations can trigger or promote self-association of MBP.

During compaction of myelin, the opposing leaflets of the cytoplasmic membrane come together to form the major dense lines, the site of MBP localization. The correspondence between the known distance of 30 Å separating the opposing cytoplasmic leaflets (Kirschner et al., 1984) and the molecular dimensions of 15 by 150 Å derived from low-angle X-ray scattering for MBP in solution (Epand et al., 1974) prompts the suggestion that two molecules of MBP can bridge the inner membrane leaflets that make up the major dense line (Golds & Braun, 1978). The observations reported here extend such a view in that the distinct lability of MBP to changes in ionic composition of the surrounding medium and the electrolyte-induced increase in self-association provide one plausible step through which myelin compaction occurs following expression of the protein.

Finally, myelin basic protein is one member of a major group of proteins that includes proteolipid protein (PLP) and protein zero (P_0) and that are present in myelin and mediate formation and compaction. While these proteins are structurally distinct and arise from separate genes, they share the common feature of possessing highly basic cytoplasmic domains (Lemke, 1988) that, in addition, show a considerable degree of amino acid sequence homology (Lees & Brostoff, 1984; Lees et al., 1984). As such, the behavior observed for MBP may provide a useful motif for analyzing the structure and function of the cytoplasmic domains of PLP and P_0. Indeed, heterodimeric interactions are known between, for example, PLP and myelin basic protein (Edwards et al., 1989).

Registry No. NATA, 2382-79-8; Trp, 73-22-3; acrylamide, 79-06-1.

REFERENCES

Azumi, T., & McGlynn, S. P. (1962) *J. Chem. Phys. 37*, 2413–2420.

Baldwin, G. S., & Carnegie, P. R. (1971) *Biochem. J. 123*, 69–74.

Ballanyl, K., & Kettenmann, H. (1990) *J. Neurosci. Res. 26*, 455–460.

Berman, H. A., & Stengle, T. R. (1975a) *J. Phys. Chem. 79*, 1001–1005.

Berman, H. A., Yeh, J. C., & Stengle, T. R. (1975b) *J. Phys. Chem. 79*, 2551–2555.

Brostoff, S. W. (1984) in *Myelin* (Morrell P., Ed.) pp 405–439, Plenum Press, New York.

Campagnoni, A. T., & Macklin, W. B. (1988) *Mol. Neurobiol. 2*, 41–89.

Chen, L. X.-Q., Petrich, J. W., Fleming, G. R., & Perico, A. (1987) *Chem. Phys. Lett. 139*, 55–61.

Chen, R. F. (1972) *J. Res. Natl. Bur. Stand., Sect. A 76*, 593–606.

Chen, R. F., & Bowman, R. L. (1965) *Science 147*, 729–732.

de Ferra, F., Engh, H., Hudson, L., Kamholtz, J., Puckett, C., Molineaux, S., & Lazzarini, R. A. (1985) *Cell 43*, 721–727.

Deibler, G. E., Boyd, L. F., & Kies, M. W. (1984) *Neurochem. Res. 9*, 1371–1385.

Edwards, A. M., Ross, N. W., Ulmer, J. B., & Braun, P. E. (1989) *J. Neurosci. Res. 22*, 97–102.

Eftink, M. R., & Ghiron, C. A. (1976) *Biochemistry 15*, 672–680.

Eftink, M. R., & Ghiron, C. A. (1981) *Anal. Biochem. 114*, 199–227.

Eftink, M. R., & Hagaman, K. A. (1986) *Biophys. Chem. 25*, 277–282.

Epand, R. M., Moscarello, M. A., Zierenberg, B., & Vall, W. J. (1974) *Biochemistry 13*, 1264–1267.

Eylar, E. H., & Thompson, M. (1969) *Arch. Biochem. Biophys. 129*, 468–479.

Golds, E., & Braun, P. (1978) *J. Biol. Chem. 253*, 8171–8177.

Gow, A., & Smith, R. (1989) *Biochem. J. 257*, 535–540.

Grinvald, A., & Steinberg, I. K. (1974) *Anal. Biochem. 59*, 583–598.

Hung, T. C., & Rauch, H. C. (1980) *Mol. Immunol. 17*, 527–531.

Kamholz, J., de Ferra, F., Puckett, C., & Lazzarini, R. (1986) *Proc. Natl. Acad. Sci. U.S.A. 83*, 4962–4966.

Kamholz, J., Toffenetti, J., & Lazzarini, R. A. (1988) *J. Neurosci. Res. 21*, 62–70.

Kettenmann, H. (1987) *Can. J. Physiol. Pharmacol. 65*, 1033–1037.

Kettenmann, H., Sonnhof, U., & Schachner, M. (1983) *J. Neurosci. 3*, 500–505.

Kirschner, D., Ganser, A. L., & Caspar, D. L. D. (1984) in *Myelin* (Morrell, P., Ed.) pp 51–95, Plenum Press, New York.

Krigbaum, W. R., & Hsu, T. S. (1975) *Biochemistry 14*, 2542–2546.

Laemmli, U. K. (1971) *Nature 270*, 680–685.

Lakowicz, J. R., Maliwal, B. P., Cherek, H., & Balter, A. (1983) *Biochemistry 22*, 1741–1752.

Lampe, P. D., Wei, G. J., & Nelsestuen, G. L. (1983) *Biochemistry 22*, 1594–1599.

Lees, M. B., & Brostoff, S. W. (1984) in *Myelin* (Morrell, P., Ed.) pp 197–224, Plenum Press, New York.

Lees, M. B., Samiullah, M., & Laursen, R. A. (1984) in *Experimental Allergic Encephalomyelitis: A Useful Model for Multiple Sclerosis* (Alvord, E. C., Jr., Kies, M. W., & Suckling, A. J., Eds.) pp 257–264, Alan R. Liss, New York.

Lehrer, S. S., & Leavis, P. C. (1978) *Methods Enzymol. 49*, 222–236.

Lemke, G. (1988) *Neuron 1*, 535–543.
Martenson, R. E., Law, M. J., & Deibler, G. E. (1983) *J. Biol. Chem. 258*, 930–937.
McCammon, J. A., & Harvey, S. C. (1987) in *Dynamics of Proteins and Nucleic Acids*, pp 25–34, Cambridge University Press, Great Britain.
Miyake, M. (1975) *J. Neurochem. 24*, 909–915.
Moskaitis, J. E., Shriver, L. C., & Campagnoni, A. T. (1987) *Neurochem. Res. 12*, 409–417.
Munro, I., Pecht, I., & Stryer, L. (1979) *Proc. Natl. Acad. Sci. U.S.A. 76*, 56–60.
Nowak, M. W., & Berman, H. A. (1991) *Biophys. J. 58*, 361a.
Record, M. T., Jr., Anderson, C. F., & Lohman, T. M. (1978) *Q. Rev. Biophys. 11*, 103–178.
Robbins, R. J., Fleming, G. R., Beddard, G. S., Robinson, G. W., Thistlewaite, P. J., & Woolfe, G. J. (1980) *J. Am. Chem. Soc. 102*, 6271–6279.
Ross, J. B. A., Roussiang, K. W., & Brand, L. (1981) *Biochemistry 20*, 4361–4369.
Shizuka, H., Serizawa, M., Shimo, T., Saito, I., & Matsuura, T. (1988) *J. Am. Chem. Soc. 110*, 1930–1934.
Smith, R. (1980) *Biochemistry 19*, 1826–1831.
Smith, R. (1985) *FEBS Lett. 183*, 331–334.
Yguerabide, J. (1972) *Methods Enzymol. 26*, 498–578.
Young, P. R., Vacante, D. A., & Snyder, W. R. (1982) *J. Am. Chem. Soc. 104*, 7287–7291.
Young, P. R., Vacante, D. A., & Waickus, C. M. (1987) *Biochim. Biophys. Acta 145*, 1112–1118.